

# Modeling Research on Flutter Characteristics of Wrap-Around Fins

Lei Zhang, Min Gao, Bukui Zhou, Limei Wang

**Abstract**—The two dimensional (2D) equations of motion for wrap-around fins (WAF), coupled with flutter and pitch, were derived by using the Lagrange method. The nonlinear aerodynamic forces of WAF were proposed based on the two-order piston theory. According to the strain expression of unilateral fixation cylindrical shell, the stiffness coefficient of WAF's imaginary torsion spring is deduced based on the energy equivalent method. Additionally, the aeroelastic model is established. Based on this, the flutter characteristics of a single WAF were studied. The results show that the fluttering speed of WAF with the variation of various parameters is approximately the same as that of the straight wing having the same projected area. However, the former is slightly higher than the latter. The fluttering speed of WAF increases linearly with the increase in thickness, decreases in the index with the increase in chord length, and first increases and then decreases with the change in the position of elastic axis. When the radian and radius are small, the fluttering speed does not change much. However, when the value exceeds a certain value, the fluttering speed increases rapidly. A certain WAF model was taken as an example, and numerical simulations were performed. It was found that the vibration divergence in the flutter direction was severer than the pitch direction. Therefore, the influence of parameters involving the flutter direction should be considered in the structural design.

**Index Terms**—Wrap-around fin; 2D wing; Flutter; Aeroelastic model; Nonlinearity

## I. INTRODUCTION

WAF is a special airfoil designed for the barrel launcher, and has been widely used in various types of rocket launchers and missiles due to its appearance that renders it specific structural advantages. However, due to a series of stability problems caused by the asymmetry of its structure, the flight instability issues of WAF missiles have occurred quite frequently [2-4].

Many scholars have studied the divergence of such movements by analyzing the flight process aerodynamic characteristics [5-8]. However, considering WAF as a cylindrical shell structure, a complex deformation response will occur under aerodynamic load, which in turn will affect the aerodynamic force on the wing. Therefore, it is necessary

to consider WAF as an aeroelastic system, and analyze its flutter characteristics under the joint action of aerodynamic force, inertial force and elastic force for the stability of this type of missile.

There is relatively little research on the aeroelastic flutter problem of large open cylindrical shells. Anderson [9,10] used the Galerkin method to analyze the flutter boundary of a cylindrical shell element. Bein [11,12] studied the nonlinear flutter problem of orthotropic flat shells, and obtained the limit cycle flutter amplitude value through direct integration. Algazin [13] used the finite difference method to solve the aerodynamic flutter boundary and modal of a cylindrical shell under arbitrary airflow decline. Wang [14] used the spline finite mode method and substructure method to study the flutter boundary of prismatic shell, compared the results with the existing analysis results and reported the verified accuracy and precision of the method. Azzouz [15,16] used the finite element method to solve the nonlinear flutter problem of a class of cylindrical flat shells with airflow decline, and solved the modal, frequency and amplitude of the flutter. Kumar [17] studied the vibration and stability of laminated double-curved shells under non-uniform load using the finite element method. Based on multi-field stratification theory, Oh [18] studied the critical dynamic pressure of piezoelectric cylindrical flat shell by considering the aerodynamic, thermal and piezoelectric effects. Shin [19] used the finite element method to study the flutter boundary and modes of composite viscoelastic cylindrical flat shells, and compared the effects of different layup methods on the results. Singha [20] used 16-node degenerating shell elements to study the effects of curvature, layering, airflow direction and boundary conditions on the flutter characteristics of cylindrical flat shells. In short, for the aeroelastic flutter problem of cylindrical shells, most of the researchers have used numerical methods to solve the problem, which is a complicated method to apply to aeroelastic engineering design. Therefore, it is necessary to seek a relatively simple analysis method for solving this issue.

Based on the simplicity of open cylindrical shell structure deformation model, the WAF model with two degrees of freedom including flutter and pitch is proposed in this work. According to the piston theory, the unsteady aerodynamic force on the wing is solved, and a 2D WAF flutter model is established. Additionally, the analysis of WAF's flutter characteristics is also conducted in this paper.

## II. OPEN CYLINDRICAL SHELL DEFORMATION MODEL

The open cylindrical shell model is constructed as shown in Figure 1. The radian is set to be  $\phi_0$ , whereas the length of chord is  $c$ . The bus on the middle surface is represented by

Manuscript received February 12, 2019; revised November 19, 2020.

Lei Zhang is an engineer of Defense Engineering, AMS, PLA, BeiJing, 100036, China (e-mail: oeczi99@163.com).

Min Gao is a professor of Army Engineering University, Shijiazhuang, Hebei, 050003, China (e-mail: gaomin1103@yeah.net).

Bukui Zhou is a senior engineer of Defense Engineering, AMS, PLA, BeiJing, 100036, China (corresponding author, e-mail: zbk751225@sina.com)

Limei Wang is a senior engineer of Defense Engineering, AMS, PLA, BeiJing, 100036, China (e-mail: 84505700@qq.com)

$x$ , whereas the circumference is given by:  $s = \varphi \cdot R$ . Furthermore,  $R = r + b/2$ , which represents the radius of curvature along the direction of circumference. In this correlation,  $r$  is the radius of missile and  $b$  is the thickness of wing. The elastic modulus is given by  $E$ , while the Poisson's ratio is  $\mu$ . The dimensionless coordinate parameters are given by:  $\alpha = x/R$ ,  $\beta = \varphi$ . The load concentrations along the bus and circumference directions were ignored. The load concentration normal to the middle surface is  $q_n$ .

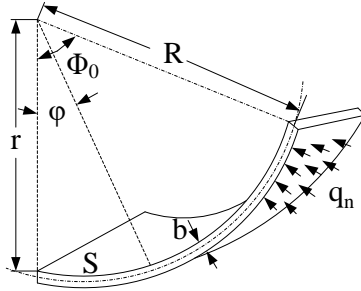


Fig.1 Cylindrical shell model

Auxiliary function  $\Phi(\alpha, \beta)$  is introduced, which represents the relationship among displacements  $u$ ,  $v$  and  $w$  along the directions of  $x$ ,  $s$  and normal to the middle surface, respectively. They are represented using Equation (1).

$$\begin{cases} u = \frac{\partial^3 \Phi}{\partial \alpha \partial \beta^2} - \mu \frac{\partial^3 \Phi}{\partial \alpha^3} \\ w = \nabla^2 \nabla^2 \Phi \\ v = -(2 + \mu) \frac{\partial^3 \Phi}{\partial \alpha^2 \partial \beta} - \frac{\partial^3 \Phi}{\partial \beta^3} \end{cases} \quad (1)$$

According to the cylindrical shell simplification theory, the deformation problem can be solved by solving the following eight-order partial differential equations under given boundary conditions (Equation (2)) [8].

$$\nabla^2 \nabla^2 \nabla^2 \nabla^2 \Phi + \frac{\partial^4 \Phi}{\partial \alpha^4} = \frac{R^2}{Eb} q_n \quad (2)$$

The boundary condition of the WAF structure is unilaterally clamped, and the remaining three sides are free. This is expressed by the auxiliary function using Equations (3) – (5).

$$\begin{cases} \frac{\partial^3 \Phi}{\partial \alpha \partial \beta^2} - \mu \frac{\partial^3 \Phi}{\partial \alpha^3} = 0 \\ (2 + \mu) \frac{\partial^3 \Phi}{\partial \alpha^2 \partial \beta} + \frac{\partial^3 \Phi}{\partial \beta^3} = 0 \\ \frac{\partial^4 \Phi}{\partial \alpha^4} + 2 \frac{\partial^4 \Phi}{\partial \alpha^2 \partial \beta^2} + \frac{\partial^4 \Phi}{\partial \beta^4} = 0 \\ \frac{\partial^5 \Phi}{\partial \alpha^4 \partial \beta} + 2 \frac{\partial^5 \Phi}{\partial \alpha^2 \partial \beta^3} + \frac{\partial^5 \Phi}{\partial \beta^5} = 0 \end{cases} \quad (3)$$

$$\begin{cases} \frac{\partial^4 \Phi}{\partial \alpha^4} = \frac{\partial^4 \Phi}{\partial \alpha^3 \partial \beta} = 0 \\ \frac{\partial^6 \Phi}{\partial \beta^6} + \frac{2 \partial^6 \Phi}{\partial \alpha^2 \partial \beta^4} + \frac{\mu \partial^6 \Phi}{\partial \alpha^2 \partial \beta^4} + \frac{\mu \partial^6 \Phi}{\partial \alpha^6} = 0 \\ \frac{\partial^7 \Phi}{\partial \beta^7} + \frac{(4 - \mu) \partial^7 \Phi}{\partial \alpha^2 \partial \beta^5} + \frac{(2 - \mu) \partial^7 \Phi}{\partial \alpha^6 \partial \beta} = 0 \end{cases} \quad (4)$$

$$\begin{cases} \frac{\partial^4 \Phi}{\partial \alpha^2 \partial \beta^2} = \frac{\partial^6 \Phi}{\partial \alpha^6} + \frac{(2 + \mu) \partial^6 \Phi}{\partial \alpha^4 \partial \beta^2} + \frac{(1 + 2\mu) \partial^6 \Phi}{\partial \alpha^2 \partial \beta^4} + \mu \frac{\partial^6 \Phi}{\partial \beta^6} = 0 \\ \frac{12(1 + \mu) R^2 \partial^4 \Phi}{b^2 \partial \alpha^3 \partial \beta} + \frac{\partial^6 \Phi}{\partial \alpha^5 \partial \beta} + \frac{\partial^6 \Phi}{\partial \alpha^3 \partial \beta^3} + \frac{\partial^6 \Phi}{\partial \alpha \partial \beta^5} = 0 \\ \frac{\partial^7 \Phi}{\partial \beta^7} + \frac{(5 - 2\mu) \partial^7 \Phi}{\partial \alpha^3 \partial \beta^4} + \frac{(4 - \mu) \partial^7 \Phi}{\partial \alpha^5 \partial \beta^2} + \frac{(2 - \mu) \partial^7 \Phi}{\partial \alpha^6 \partial \beta} = 0 \end{cases} \quad (5)$$

$\Phi(\alpha, \beta)$  can be solved using Equations (2) – (5). Then, the displacements  $u$ ,  $v$ , and  $w$  can be obtained. According to the moment theory of cylindrical shell [8], the three strain components in the middle surface are given by Equation (6).

$$\begin{cases} \varepsilon_\alpha = \frac{\partial u}{\partial x} \\ \varepsilon_\beta = \frac{1}{R} \frac{\partial v}{\partial \varphi} + \frac{w}{R} \\ \gamma_{\alpha\beta} = \frac{1}{R} \frac{\partial u}{\partial \varphi} + \frac{\partial v}{\partial x} \end{cases} \quad (6)$$

The changes in curvature and twist rate are given by Equation (7).

$$\begin{cases} \kappa_1 = -\frac{\partial^2 w}{\partial x^2} \\ \kappa_2 = -\frac{1}{R^2} \frac{\partial^2 w}{\partial \varphi^2} - \frac{w}{R^2} \\ \chi = \frac{1}{2R} \left( \frac{\partial v}{\partial x} - \frac{1}{R} \frac{\partial u}{\partial \varphi} - 2 \frac{\partial^2 w}{\partial x \partial \varphi} \right) \end{cases} \quad (7)$$

However, while solving this model, it is difficult to find a certain form of the auxiliary function that meets all the boundary conditions, which means that the above equation can only be solved by numerical methods. It is impossible to qualitatively analyze the chatter characteristics of systems with different parameters without analytical expressions. Therefore, it is necessary to find a relatively succinct alternative model for subsequent theoretical research.

### III. TWO-DEGREE-OF-FREEDOM WAF MODEL

In the case of small disturbances, the displacements of the points on WAF can be represented by the two degrees of freedom of flutter and pitch [21]. Assume that, there are two springs, which have the imaginary stiffnesses of  $K_\kappa$  and  $K_\theta$ . At the base of the fins, two degrees of freedom, namely the flutter  $\kappa$  and pitch  $\theta$  are introduced.

### A. Free vibration model

In order to simplify the research process, the influence of open angles is ignored. The arc radius of WAF is represented by  $\phi_0$ , whereas the medium radius of the curve is represented by  $r$ . Furthermore, the chord length is represented by  $c$ . The aerodynamic center is located at the  $1/4$  of chord length and the elastic axis is located behind it  $ec$ , as shown in Figure 2.

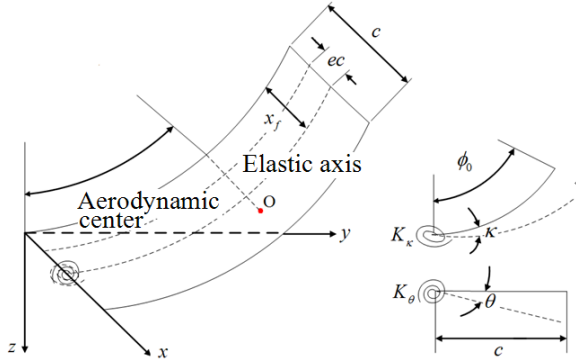


Fig.2 WAF model

The displacement of a certain point O on the wing in its normal direction can be expressed using Equation (8).

$$z(x, \alpha, t) = 2r \sin \frac{\alpha}{2} \cdot \kappa(t) + (x - x_f) \cos \alpha \cdot \theta(t) \quad (8)$$

Therefore, the kinetic energy of WAF is given by Equation (9).

$$T = \int_0^c \int_0^{\phi_0} \frac{1}{2} m r z^2 d\alpha dx \quad (9)$$

where  $m$  represents the mass per unit area.

Spring strain energy is given by Equation (10).

$$U = \frac{1}{2} K_\kappa \kappa^2 + \frac{1}{2} K_\theta \theta^2 \quad (10)$$

The free vibration model of WAF can be obtained by applying the Lagrange equations to the generalized coordinates  $\kappa$  and  $\theta$ , respectively (see Equation (11)).

$$A \cdot \begin{Bmatrix} \ddot{\kappa} \\ \ddot{\theta} \end{Bmatrix} + D \cdot \begin{Bmatrix} \dot{\kappa} \\ \dot{\theta} \end{Bmatrix} = \begin{Bmatrix} 0 \\ 0 \end{Bmatrix} \quad (11)$$

where the inertia matrix  $A = \begin{bmatrix} I_\kappa & I_{\kappa\theta} \\ I_{\kappa\theta} & I_\theta \end{bmatrix}$ , elastic

$$\text{matrix } D = \begin{bmatrix} K_\kappa & 0 \\ 0 & K_\theta \end{bmatrix}.$$

$I_\kappa$ ,  $I_\theta$ , and  $I_{\kappa\theta}$  represent the flutter inertia moments, pitch inertia moments and inertial products, respectively, and are given by Equations (12) – (14).

$$I_\kappa = 2mr^3 c (\phi_0 - \sin \phi_0) \quad (12)$$

$$I_\theta = \frac{1}{12} mr [(c - x_f)^3 + x_f^3] \cdot (\sin 2\phi_0 + 2\phi_0) \quad (13)$$

$$I_{\kappa\theta} = mr^2 (c^2 - 2cx_f) \left( 2 \cos \frac{\phi_0}{2} - \frac{4}{3} \cos^3 \frac{\phi_0}{2} - \frac{2}{3} \right) \quad (14)$$

### B. Generalized force solution based on piston theory

For Point O, the wash speeds of upper and lower airfoils are given by Equation (15).

$$V_{u,l} = \pm \left( V \frac{\partial}{\partial x} + \frac{\partial}{\partial t} \right) z(x, \alpha, t) \quad (15)$$

According to the second-order piston theory, the pressure difference between the upper and lower surfaces of Point O is given by Equation (16).

$$\begin{aligned} \Delta p(x, \alpha, t) &= p_l - p_u = \rho_\infty \gamma \left[ \frac{1}{c_\infty} (V_l - V_u) + \frac{(\gamma + 1)}{4c_\infty^2} (V_l^2 - V_u^2) \right] \\ &= \frac{4q}{M_\infty V} \left[ 2r \sin \frac{\alpha}{2} \dot{\kappa}(t) + (x - x_f) \cos \alpha \dot{\theta}(t) + V \cos \alpha \theta(t) \right] \end{aligned} \quad (16)$$

where  $q = \frac{1}{2} \rho_\infty V^2$  and represents the dynamic pressure of air.

Then, the aerodynamic force and aerodynamic torque on the wing could be solved (see Equations (17) and (18)).

$$\begin{aligned} L &= \int_0^c \int_0^{\phi_0} \Delta p(x, \alpha, t) dx d\alpha = \frac{4qc}{M_\infty V} \left[ -4r \cos \frac{\phi_0}{2} \dot{\kappa}(t) + \left( \frac{c^2}{2} - cx_f \right) \sin \phi_0 \dot{\theta}(t) + V \sin \phi_0 \theta(t) \right] \end{aligned} \quad (17)$$

$$\begin{aligned} M &= \int_0^c \int_0^{\phi_0} \Delta p(x, \alpha, t) (x - x_f) dx d\alpha = \frac{4qc}{M_\infty V} \left[ \left( \frac{c}{2} - x_f \right) (V \sin \phi_0 \theta(t) - 4r \cos \frac{\phi_0}{2} \dot{\kappa}(t)) + \left( \frac{c}{3} - \frac{2}{3} x_f - x_f^2 \right) \sin \phi_0 \dot{\theta}(t) \right] \end{aligned} \quad (18)$$

When the generalized coordinates  $\kappa$  and  $\theta$  have increments of  $\delta\kappa$  and  $\delta\theta$ , respectively, the incremental displacements at Point O are given by Equations (19) and (20).

$$dz_\kappa = 2r \sin \frac{\alpha}{2} \cdot \delta\kappa \quad (19)$$

$$dz_\theta = (x - x_f) \cos \alpha \delta\theta \quad (20)$$

Therefore, the incremental work done by the aerodynamic forces on WAF is given by Equation (21).

$$\delta W = \int_0^c \int_0^{\phi_0} -\Delta p(x, \alpha, t) (dz_\theta + dz_\kappa) dx d\alpha \quad (21)$$

Then, the generalized force can be obtained and is given by Equations (22) and (23).

$$\begin{aligned} Q_\kappa &= \frac{\partial(\delta W)}{\partial(\delta\kappa)} = -\frac{4q}{M_\infty V} \int_0^c \int_0^{\phi_0} 2r \sin \frac{\alpha}{2} \cdot [2r \sin \frac{\alpha}{2} \dot{\kappa}(t) + (x - x_f) \cos \alpha \dot{\theta}(t) + V \cos \alpha \theta(t)] dx d\alpha \\ &= -\frac{4q}{M_\infty V} \left[ 4cr^2 \left( \frac{\phi_0}{2} - \frac{\sin \phi_0}{2} \right) \dot{\kappa}(t) + 2r \left( \frac{1}{2} c^2 - cx_f \right) \left( 2 \cos \frac{\phi_0}{2} - \frac{4}{3} \cos^3 \frac{\phi_0}{2} - \frac{2}{3} \right) \dot{\theta}(t) + 2cr \left( 2 \cos \frac{\phi_0}{2} - \frac{4}{3} \cos^3 \frac{\phi_0}{2} - \frac{2}{3} \right) V \theta(t) \right] \end{aligned} \quad (22)$$

$$\begin{aligned}
 Q_o &= \frac{\partial(\delta W)}{\partial(\delta\theta)} = -\frac{4q}{M_\infty V} \int_0^c (x-x_f) \cos \alpha \cdot [2r \sin \frac{\alpha}{2} \kappa(t) + (x-x_f) \cos \alpha \theta(t) + \\
 &V \cos \alpha \theta(t)] dx d\alpha = -\frac{4q}{M_\infty V} [2r(2 \cos \frac{\phi_0}{2} - \frac{4}{3} \cos^3 \frac{\phi_0}{2} - \frac{2}{3})(\frac{1}{2}c^2 - cx_f) \kappa(t) + \\
 &(\frac{\phi_0}{2} + \frac{\sin 2\phi_0}{4})(\frac{1}{3}c^3 - x_f c^2 + x_f^2 c) \theta(t) + (\frac{\phi_0}{2} + \frac{\sin 2\phi_0}{4})(\frac{1}{2}c^2 - cx_f) V \theta(t)]
 \end{aligned} \quad (23)$$

The free-vibration model (Equation 11) is combined, and the complete flutter model could be proposed (see Equation (24)).

$$A \cdot \begin{Bmatrix} \ddot{\kappa} \\ \ddot{\theta} \end{Bmatrix} + B \cdot \begin{Bmatrix} \dot{\kappa} \\ \dot{\theta} \end{Bmatrix} + (C + D) \cdot \begin{Bmatrix} \kappa \\ \theta \end{Bmatrix} = \begin{Bmatrix} 0 \\ 0 \end{Bmatrix} \quad (24)$$

$$\text{where } B = \begin{bmatrix} b_{11} & b_{12} \\ b_{21} & b_{22} \end{bmatrix}, C = V \begin{bmatrix} 0 & c_{12} \\ 0 & c_{22} \end{bmatrix}$$

The elements are:

$$\begin{aligned}
 b_{11} &= 8\rho_\infty c_\infty r^2 \left( \frac{\phi_0}{2} - \frac{\sin \phi_0}{2} \right) \\
 b_{12} = b_{21} &= 4\rho_\infty c_\infty r \left( 2 \cos \frac{\phi_0}{2} - \frac{4}{3} \cos^3 \frac{\phi_0}{2} - \frac{2}{3} \right) \left( \frac{1}{2}c^2 - cx_f \right) \\
 b_{22} &= 2\rho_\infty c_\infty \left( \frac{\phi_0}{2} + \frac{\sin 2\phi_0}{4} \right) \left( \frac{1}{3}c^3 - x_f c^2 + x_f^2 c \right) \\
 c_{12} &= 4cr\rho_\infty c_\infty \left( 2 \cos \frac{\phi_0}{2} - \frac{4}{3} \cos^3 \frac{\phi_0}{2} - \frac{2}{3} \right) \\
 c_{22} &= 2\rho_\infty c_\infty \left( \frac{\phi_0}{2} + \frac{\sin 2\phi_0}{4} \right) \left( \frac{1}{2}c^2 - cx_f \right)
 \end{aligned}$$

### C. Stiffness coefficient solution based on energy equivalent

In the flutter model, the stiffness coefficient of imaginary torsion spring is a key parameter, which is determined by the wing shape. For straight wings, it could be calculated by the zero airspeed frequency [9], which is not applicable for WAF. Therefore, it is necessary to find an appropriate alternative method to establish the equivalent stiffness model of WAF.

In vibration theory, energy method is often used to calculate the structural equivalent stiffness. Because the WAF flutter model involves two torsion springs, and the aerodynamic load on the wing will inevitably lead to deformation in the two directions, the load should be decomposed into two components. Each component affects the displacement in one direction.

Furthermore, the aerodynamic force component along the normal direction is set to be  $q_n(\varphi)$ . The action position from the aerodynamic center to the elastic axis is translated, and defined as  $q_{n1}$ . A pair of force couples of size  $\frac{q_n(\varphi)}{2}$  is added, which acts on the aerodynamic center and the relative positions of elastic axes. They are defined as  $q_{n2}$  and  $q_{n3}$ , respectively, as shown in Figure 3.

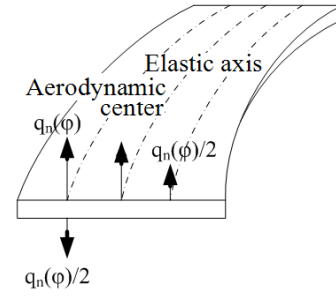


Fig.3 Aerodynamic equivalence

When considering only  $q_{n1}$ , the moment in pitch direction is zero, while the moment acting on flutter torsion spring is given by Equation (25).

$$M_p = \int_0^{\phi_0} 2R \sin \frac{\varphi}{2} \cdot q_n(\varphi) d\varphi \quad (25)$$

The elastic potential energy is given by:  $T_p = \frac{M_p^2}{2K_\kappa}$

For the cylindrical shell model, under the action of load  $q_{n1}$ , the deformation energy consists of two parts. One part corresponds to the uniform deformation energy in the direction of thickness, which is the deformation energy of the film's stress state.

$$U_1 = \frac{Eb}{2(1-\mu^2)} \iint [(\varepsilon_\alpha + \varepsilon_\beta)^2 + 2(1-\mu) \cdot (\frac{1}{4}\gamma_{\alpha\beta}^2 - \varepsilon_\alpha \varepsilon_\beta)] AB d\alpha d\beta \quad (26)$$

Another part corresponds to the bending deformation (see Equation (27)).

$$U_2 = \frac{Eb^3}{24(1-\mu^2)} \iint [(\kappa_1 + \kappa_2)^2 + 2(1-\mu) \cdot (\chi^2 - \kappa_1 \kappa_2)] AB d\alpha d\beta \quad (27)$$

The stress-strain value in the above equation can be solved numerically using Equations (6) and (7). Furthermore,  $T_p = U_1 + U_2$ , and the equivalent stiffness coefficient of fluttering spring under specific load conditions can be solved.

Similarly, considering only the couple load  $q_{n2}$  and  $q_{n3}$ , the moment in the flutter direction is zero, and the equivalent stiffness coefficient of pitching spring can be solved.

## IV. ANALYSIS OF FLUTTER CHARACTERISTICS OF WAF

### A. Flutter Critical Speed Solution

Assume that the solution of Equation (24) is given by Equation (28).

$$\begin{Bmatrix} \kappa \\ \theta \end{Bmatrix} = \begin{Bmatrix} \kappa_0 \\ \theta_0 \end{Bmatrix} e^{2t} \quad (1)$$

Suppose that

$$K_\kappa = xV, K_\theta = \mu xV \quad (29)$$

where  $\mu$  represents the ratio of two spring stiffness coefficients, and  $x$  is an unknown coefficient that needs to be solved.

If Equation (24) has a non-zero solution, then Equation (30) can be obtained.

$$\begin{vmatrix} I_{\kappa}\lambda^2 + b_{11}\lambda + xV & I_{\kappa\theta}\lambda^2 + c_{12}V \\ I_{\kappa\theta}\lambda^2 + b_{21}\lambda & I_{\theta}\lambda^2 + (c_{22} + \mu x)V \end{vmatrix} = 0 \quad (30)$$

The following quartic equation can be obtained by solving the determinant.

$$b_4\lambda^4 + b_3\lambda^3 + b_2\lambda^2 + b_1\lambda + b_0 = 0 \quad (31)$$

where

$$\begin{cases} b_4 = I_{\kappa}I_{\theta} - I_{\kappa\theta}^2 \\ b_3 = I_{\theta}b_{11} - I_{\kappa\theta}b_{21} \\ b_2 = [(\mu I_{\kappa} + I_{\theta})x + (I_{\kappa}c_{22} - I_{\kappa\theta}c_{12})]V = (p_1x + p_0)V \\ b_1 = (\mu b_{11}x + b_{11}c_{22} - b_{21}c_{12})V = (q_1x + q_0)V \\ b_0 = (\mu x^2 + c_{22}x)V^2 = (r_2x^2 + r_1x)V^2 \end{cases} \quad (32)$$

According to the Routh-Hurwitz stability criterion, the critical condition for system flutter is given by Equation (33).

$$b_4b_1^2 - b_1b_2b_3 + b_0b_3^2 = 0 \quad (33)$$

Substituting each parametric expression into the equation and eliminating the term of  $V^2$ , the quadratic equation about the unknown coefficient  $x$  can be obtained.

$$(b_4q_1^2 - b_3p_1q_1 + b_3^2r_2)x^2 + (2b_4q_1q_0 - b_3p_1q_0 - b_3p_0q_1 + b_3^2r_1)x + (b_4q_0^2 - b_3p_0q_0) = 0 \quad (34)$$

Substituting the root of this equation into Equation (29), the flutter speed could be solved.

### B. Parameter impact analysis

Obviously, the flutter speed is affected by various structural parameters. Therefore, it is necessary to analyze the variation trend of flutter speed with different parameters to provide a theoretical basis for the aerodynamic design of WAF.

Figures 4-6 show the comparison of variation in flutter speed with different structural parameters of WAF and flat wing with the equal projection area.

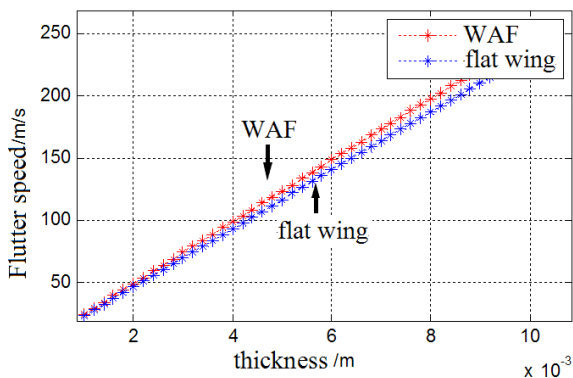


Fig.4 Flutter speed varies with thickness

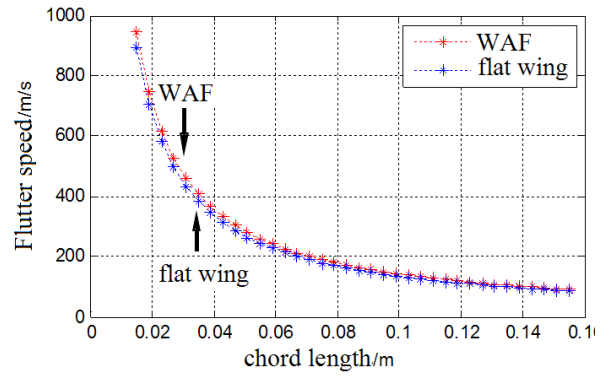


Fig.5 Flutter speed varies with chord length

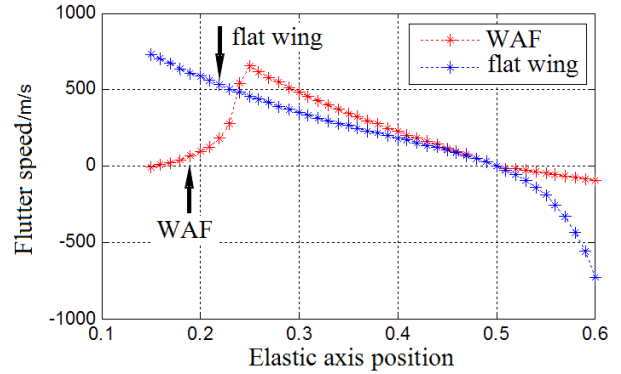


Fig-6 Flutter speed varies with Elastic axis position

Based upon numerical simulation results, following observations can be made.

1. The variation trends of flutter speed of the two kinds of wings are almost the same. However, the flutter speed of WAF is slightly higher than the flat wing. Therefore, in terms of the flutter stability of a single wing, WAF is better than the flat tail.

2. Flutter speed increases linearly with the increase in thickness, which means that increasing the thickness is an effective way to improve the stability of WAF.

3. Flutter speed decreases in the index with the increase of chord length. Obviously, under the premise of ensuring sufficient lift area, shorter the design chord length, better is the stability.

4. The variations in flutter speeds with the change in position of the elastic axis of the two kinds of wings are obviously different. The flutter speed of flat wing flutter monotonously decreases, while that of the WAF first increases, and then, decreases. Therefore, in the structural design, the position of the elastic axis should be as close to the "extreme point" as possible.

Fig. 7 and Fig. 8 show the variation curves of the flutter speed with radian and radius of WAF.

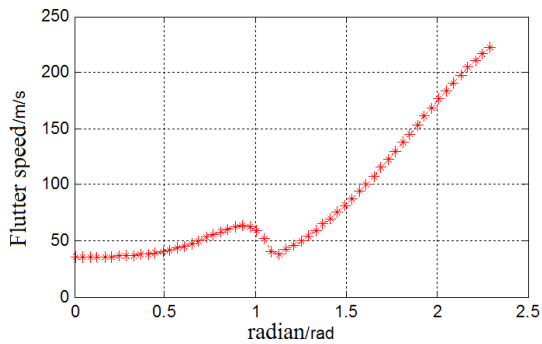


Fig.7 Flutter speed varies with radian

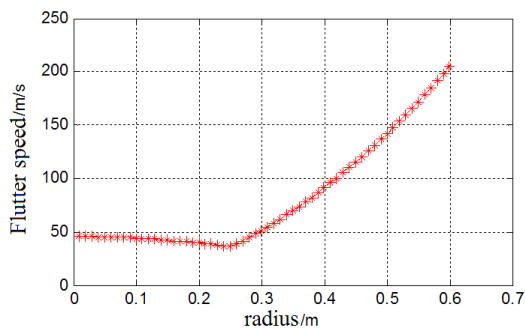


Fig.8 Flutter speed varies with winding radius

It can be seen that the flutter speed does not change much, but only slightly increases or decreases before the two parameters increase from zero to a certain point. However, after that point, the fluttering speed increases sharply.

In fact, for the WAF design of a certain projectile type, the caliber is determined, and the arc is also decided by the number of wings. Therefore, more attention is paid to the influence of chord length and position of elastic axis on the flutter speed. Figure 9 shows the variation of flutter speed with the two factors.

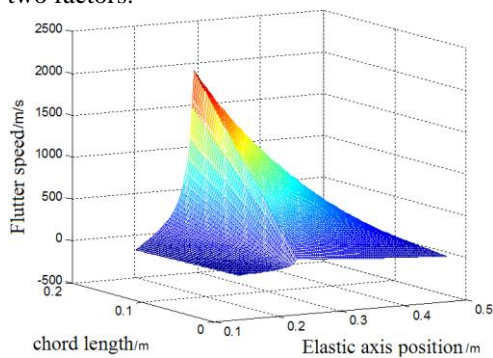


Fig.9 Flutter speed varies trend

C. Case study

Take a specific WAF model as an example. The structural parameters are as follows.

Tab.1 Model structure parameters

$\phi_0$	1.57rad	Aerodynamic center position	0.25c
$r$	0.061m	Elastic axis position	0.45c
$c$	0.155m	$K_x$	1.879 N·m/rad
$d$	0.006m	$K_\theta$	2.795 N·m/rad
	$7.9 \times 10^3 \text{kg/m}^3$	Lift line slope	5.73

According to the Routh-Hurwitz method, the flutter speed of model is 79.48 m/s.

Under the condition that the initial values of pitch and flutter were all taken to be 0.004 rad, the dynamic responses of WAF at the airspeeds of 75 m/s, 80 m/s, 85 m/s, 90 m/s, and 100 m/s Figures 10 – 14, respectively.

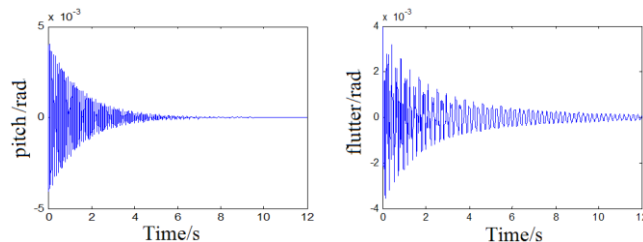


Fig.10 Timing response of tail vibration under 75m/s speed

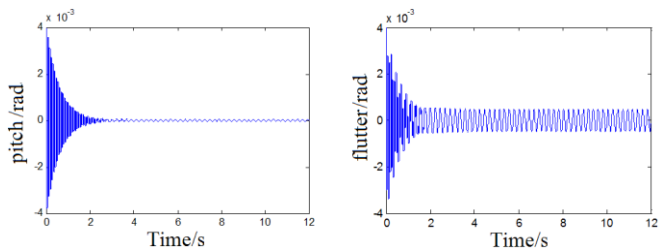


Fig.10 Timing response of tail vibration under 80m/s speed

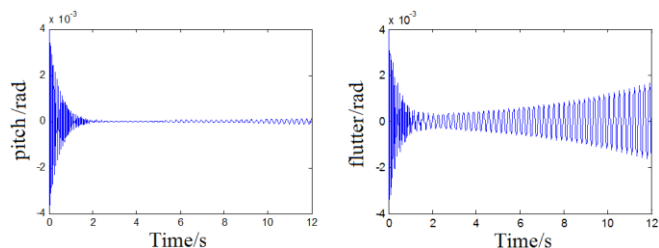


Fig.11 Timing response of tail vibration under 85m/s speed

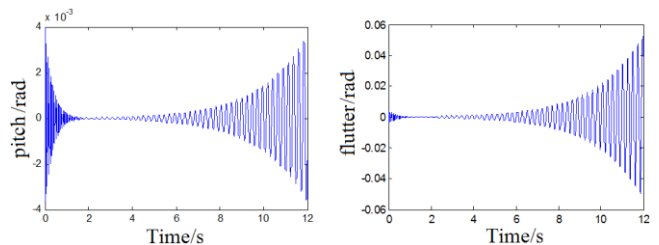


Fig.12 Timing response of tail vibration under 90m/s speed

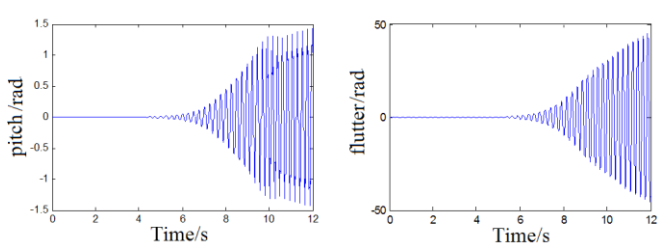


Fig.13 Timing response of tail vibration under 100m/s speed

When the airspeed is lower than the flutter speed, the vibration decays exponentially due to the action of aerodynamic damping. When the airspeed reaches the critical flutter speed, WAF makes a simple harmonic vibration. As the airspeed continues to increase, the vibration presents a divergent trend.

It is easy to observe that the vibration divergence in the pitch direction is significantly weaker than that in the flutter direction. Therefore, in the structural design, the influence of parameters related to flutter direction on the flutter speed must be emphasized.

## V. CONCLUSIONS

In this paper, the aeroelastic model of WAF, which involved two degrees of freedom, namely the flutter and pitch, is established by simplifying the vibration form of cylindrical shell. Based on this model, the flutter characteristics of WAF were analyzed, which showed that the aeroelasticity of WAF is slightly better than that of the flat wing with the equal projection area. Variation of flutter speed with different structural parameters was studied, which provides a theoretical basis for the aeroelastic design of WAF. The numerical simulations of a certain WAF model were carried out, which showed that the vibration divergence in the pitch direction is significantly weaker than that in the flutter direction.

It should be pointed out that in order to simplify the research process, the model established in this paper does not consider the impact of ballistic rolling. The existing research shows that the out-of-plane force and moment generated by missile rolling are important factors affecting the flight stability. In addition, nonlinear factors have an important impact on the motion response of aeroelastic systems [22, 23], while gap nonlinearities are common in the wrap-around fins. Therefore, it is necessary to study these factors in future works.

## REFERENCES

- [1] Miao Ruisheng, Ju Xianming, Wu Jiasheng. Missile Aerodynamics [M]. National Defense Industry Press, 2006
- [2] Curry W H, Reed J F. Measurement of magnus effects on a sounding rocket model in a supersonic wind tunnel [R]. AIAA-66-754. 1966
- [3] Nicolaides J D, Ingram C W, Clare T A. An investigation of the non-linear flight dynamics of ordnance weapons[R]. AIAA- 69-135. 1969
- [4] Liano M G. Stability analysis and flight trials of a clipped wrap around fin configuration, [R]. AIAA-2004-5055. 2004
- [5] WANG Hua-bi, WU Jiasheng. Coning motion of Rocket, Its Numerical Simulation and Restraint.[J] Transactions of Beijing Institute of Technology, 2007,27(3):196-199.
- [6] LEI Juanmian, Wu Jiasheng. Coning motion and restraint of large fineness ratio unguided spinning rocket stabilized with tail fin [J]. Acta Aerodynamic Sinica, 2005, 23(4): 455-457.
- [7] ZHAO Liangyu, YANG Shu-xing, JIAO Qing-jie Several Methods for Improving Asymptotic Stability of Coning Motion of Wrap-around-fin Rockets [J]. Journal of Solid Rocket Technology, 2010,33(4): 369-372.
- [8] ZHAO Liang-yu, YANG Shu-xing, JIAO Qing-jie. Research on Convergence Speed of Coning Motion of Wrap-around-fin Rocket [J]. Journal of Solid Rocket Technology, 2009, 32(1): 15-19.
- [9] Anderson, W. J, Panel flutter of cylindrical shells, Final report of ORA project 08079,NASA NGR-23-005-166, 1967.
- [10] Anderson W. J., Kuo-Hsiung Hsu, Engineering estimates for supersonic flutter of curved shell segments, AIAA J, 1970 8(3):446-451.
- [11] Bein T., Friedmann P. P., Zhong X., Nydick I., Hypersonic flutter of a curved shallow panel with aerodynamic heating, Proceedings of the 34th AIAA/ASME/ASCE/AHS/ASC Structures, Structural Dynamics and Materials Conference, 1993, La Jolla, California, PI-15(AIAAPaper93-1318).
- [12] Nydick I., Friedmann P. P., Zhong X., Hypersonic Panel flutter studies on curved Panels, Proceedings of the 36<sup>th</sup> AIAA/ASME/ASCE/AHS/ASC Structures, Structural Dynamics and Materials Conference, 1995, New Orleans, 5:2995-3011 (AIAA Paper 95-1485-CP).
- [13] Algazin S. D, Kiyko I. A, Numerical analysis of the flutter of a shallow shell, Journal of Applied Mechanics & Technical Physics 1999, 40(6):1082-1087.
- [14] Wang S, High-supersonic/hypersonic flutter of prismatic composite plate/shell panels, Journal of Spacecraft & Rockets, 1999, 36(5):750-757.
- [15] Azzouz, M. S, Guo, X., Przekop, A., Mei, C., Nonlinear flutter of cylindrical shell Panels under yawed supersonic flow using FE, 45<sup>th</sup> AIAA/ASME/ASCE/AHS/ASC Structure, Structural Dynamics & Materials Conference, 2004, Palm Springs, California, AIAA 2004-2043.
- [16] Azzouz, M. S, Flow angle effects on supersonic flutter of curved Panels, Proceedings of The 2008 IAJC-IJME International Conference, 019.
- [17] Kumar, L.R, Datta, P. K, Prabhakara, D. L, Dynamic instability characteristics of laminated composite doubly curved panels subjected to partially distributed follower edge loading, International Journal of Solids & Structure, 2005, 42:2243-2264.
- [18] Oh, I. K, Lee I, Supersonic flutter suppression of piezolaminated cylindrical panels based on multifield layerwise theory, Journal of Sound & Vibration, 2006, 291:1186-1201.
- [19] Won-Ho Shin, Aeroelastic characteristics of cylindrical hybrid composite panels with viscoelastic damping treatments, Journal of Sound & Vibration, 2006, 296: 99-116.
- [20] Singha M. K, Mandal M, Supersonic flutter characteristics of composite cylindrical panels, Composite Structures, 2008, 82(2):295-301.
- [21] J.R.Wright, J.E. Cooper. Introduction to Aircraft Aeroelasticity and Loads [M]. Shanghai Jiaotong University Press. 2010
- [22] Zhao Hai,Cao Deng-qing. Aerodynamic flutter and limited cycle of a 2-D wing in the supersonic flow field [C]. The 12th National Conference on Nonlinear Vibration, 2009: 767-772
- [23] ZHENG Guo-yong, YANG Yi-ren. Complicated Response of A 2-D Wing with Structural Nonlinearity in Supersonic Flow [J]. Journal of Vibration and Shock, 2007,26(12):96-100.